Available online at www.sciencedirect.com
SCIENCE DIRECT®
International Journal of Heat and Fluid Flow 25 (2004) 618–624
International Journal of HEAT AND FLUID FLOW
www.elsevier.com/locate/ijhff

On the drag reduction mechanism in a lubricated turbulent channel flow

Stian Solbakken, Helge I. Andersson *

Department of Energy and Process Engineering, Norwegian University of Science and Technology, K. Hejes vei 2, N-7491 Trondheim, Norway

Received 27 June 2003; accepted 6 March 2004
Available online 20 May 2004

Abstract

Turbulent flow in a lubricated plane channel has been considered. Direct numerical simulations showed that a substantial drag reduction can be achieved when thin films are lubricating the channel walls. The wall-normal velocity is suppressed inside the lubricating film, whereas planar fluid motions prevail. The bulk fluid is no longer exposed to no-slip at the solid surfaces, but the turbulence statistics and the coherent near-wall structures nevertheless closely resemble those observed in a dry channel. It is concluded that the interface between the bulk-fluid and the more viscous lubricating layer acts as an insulator which hinders the intense downwash of high-speed fluid, caused by the coherent vortices, to hit the solid surface.

PACS: 42.27.Lx
Keywords: Drag reduction; Channel flow; Turbulence; Direct numerical simulation; Lubrication

1. Introduction

In recent years numerous strategies have been developed in order to control turbulent boundary layers and other wall-bounded flows, particularly with an objective to achieve skin-friction drag reduction. In this context direct numerical simulations have proven to be a powerful tool for exploring the physical mechanisms that determine the skin-friction level. It is now known that the streamwise vortices in the near-wall region are responsible for a major part of the production of turbulent stresses (Jeong et al., 1997; Robinson, 1991) through the celebrated sweep and ejection events and, ultimately, for the excess skin-friction in turbulent flows. These near-wall vortical structures are associated with local high-skin-friction regions (Choi et al., 1993; Kravchenko et al., 1993; Solbakken and Andersson, 2004) created by the inrush of high-speed fluid induced by the streamwise vortices. Consequently, most attempts for obtaining skin-friction reduction have focused on either directly suppressing the strength of the streamwise vortices in the buffer layer or by regulating their effect on the wall. Kim (1992) has proposed the near-wall streamwise vortices to be the single most important turbulent structure from the perspective of drag manipulation.

Examples of successful strategies for skin-friction drag reduction, explored by direct numerical simulations, include riblets (Choi et al., 1993), compliant surfaces (Endo and Himeno, 2002), polymer additives (den Toonder et al., 1997; Orlandi, 1995), wall oscillations (Orlandi and Fatica, 1997), opposition control (Hammond et al., 1998; Choi et al., 1994), active wall motions (Kang and Choi, 2000), uniform blowing (Sumitani and Kasagi, 1995), body force imposed in the near-wall region (Satatke and Kasagi, 1996; Lee and Kim, 2002), neural network (Lee et al., 1997) and large-scale flow forcing (Schoppa and Hussain, 1998). The similarity between all these strategies is that skin-friction drag reduction is obtained by manipulating the near-wall streamwise vortices. However, most of these strategies are hard to implement in a real-life application.

The opposition control of Hammond et al. (1998) and Choi et al. (1994) is an active turbulence control that effectively suppresses the streamwise vortices present in

* Corresponding author. Tel.: +47-73-59-35-56; fax: +47-73-59-34-91.
E-mail address: helge.i.andersson@ntnu.no (H.I. Andersson).

0142-727X/$ - see front matter © 2004 Elsevier Inc. All rights reserved.
doi:10.1016/j.ijheatfluidflow.2004.03.001

the near-wall region. Furthermore, this control scheme creates a "virtual wall", i.e. a plane that has approximately no throughflow, close to the solid surface. This prevents high-speed fluid from interacting with the wall, and the occurrences of local high skin-friction regions are thereby obstructed. The mitigation of vertical transport of streamwise momentum will ultimately reduce the Reynolds shear-stress. As a consequence the viscous sublayer is thickened and a significant drag reduction can be observed. Unfortunately, no technology capable of performing the opposition control (Hammond et al., 1998; Choi et al., 1994) exists today, nor is it expected to be developed in the foreseeable future. Another drawback of active turbulence control is the necessity of an energy input. The existence of a "virtual wall" close to the rigid wall suggests that a fluid–fluid interface in the same region could play an analogous role and also result in a significant skin-friction drag reduction. A thin lubricating film, i.e. a thin layer of a more viscous fluid, might also be used in order to isolate the bulk-fluid from contact with the wall and thereby increase the throughput or decrease the drag. Motivated by the promising results obtained with opposition control (Hammond et al., 1998; Choi et al., 1994), the present investigation focuses on the possibility of obtaining skin-friction drag reduction when a thin lubricating film is applied at the wall.

It is well known that drag reduction can be achieved in core-annular pipe flow when the lubricant viscosity is smaller than that of the bulk fluid, see e.g. the recent review article of (Joseph et al., 1997). A prominent example is the water-lubricated pipeline transport of heavy viscous oils. More recently, (Rojey et al., 1999) suggested that drag reduction might occur in pressurised gas flow in the presence of a thin annular liquid film. In this case, which will be considered herein, the lubricant is more viscous than the core fluid and the interface is likely to be hydrodynamically unstable. The inception of surface waves will inevitably increase the pressure loss compared to that associated with a smooth (i.e. wave-free) film. Miles (1960) showed that a liquid film sheared by an adjacent gas flow is stable as long as the Weber number

$$We = \frac{\rho_{\text{film}} u_i^2 h}{\sigma} \tag{1}$$

does not exceed 3, i.e. provided that the surface tension σ suffices to prevent interfacial waves from developing. Here, ρ_{film} and h denote the density and the thickness of the liquid film and u_i is the interfacial velocity. This result was later confirmed by the somewhat improved investigation by Smith and Davis (1982). These simplified analyses have been extended throughout the years by several authors, including the more recent study by Miesen and Boersma (1995). According to these investigations the assumption of a smooth interface can be justified for sufficiently thin lubricating layers since the film Reynolds number should be low. However, infinitely thin films are hydrodynamically unstable and a wave-free interface can therefore only be achieved in a certain range of small but yet finite film thicknesses.

The present study is nothing but an idealised computer experiment in which a planar channel geometry rather than a circular pipe configuration is examined. Although most practical applications envisaged are high Reynolds number cases, only low Reynolds number cases can be considered in this study to enable direct numerical simulations to be performed. The aim is simply to demonstrate that substantial pressure loss reduction, i.e. drag reduction, can be achieved by lubrication. Furthermore, the physical mechanisms responsible for the drag reduction will be explored.

2. Problem formulation and numerical aspects

In this study direct numerical simulations of both conventional and lubricated fully developed turbulent channel flows are performed. The lubricated channel (shown in Fig. 1) is identical to the conventional channel, except for the presence of a lubricating film at both channel walls. The lubricating film has a uniform thickness of $h = H/18$, the kinematic viscosity is twice that of the bulk-fluid ($\nu_{\text{film}} = 2\nu$) and the density ratio is one ($\rho_{\text{film}} = \rho$). An impermeability condition ($v_{\text{wall–normal}} = 0$) is applied at the planar interface between the bulk-fluid and the lubricating film. Continuity of stresses ($\boldsymbol{\tau}_{\text{film}} = \boldsymbol{\tau}_{\text{bulk-fluid}}$) and velocities ($\mathbf{u}_{\text{film}} = \mathbf{u}_{\text{bulk-fluid}}$) are imposed at the interface. The Reynolds number based on the global friction velocity $u_\tau = \sqrt{\tau_{\text{wall}}/\rho}$, the bulk-fluid viscosity ν and channel half-height H is $Re_\tau = 180$ for both the lubricated and the conventional channel flow. In other words, the driving mean pressure gradient $-\mathrm{d}P/\mathrm{d}x = \tau_{\text{wall}}/H$ is the same in both simulations. In addition, an alternative lubricated channel flow simulation, in which the volumetric flow rate is kept constant, is started from an initial field taken from the conventional channel flow. This simulation is used for studying the temporal change in skin-friction

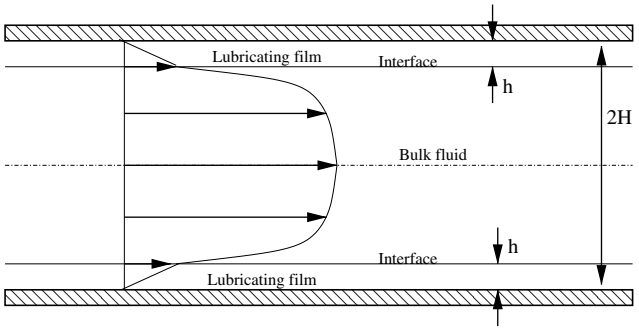

Fig. 1. The lubricated channel.

drag and is terminated when a statistically steady solution is obtained.

The computer code MGLET (Manhart et al., 2001; Orellano and Wengle, 2000) used is based on a second-order finite-volume formulation of the incompressible Navier–Stokes equations. The size of the computational domain in the streamwise (x), wall-normal (y) and spanwise (z) directions is $4\pi H \times 2H \times 2\pi H$, and the corresponding number of grid cells are $192 \times 192 \times 192$. Throughout this paper, u, v and w denote the streamwise, wall-normal and spanwise velocities, respectively. Velocity, length and time are expressed in wall units as $u^+ = u/u_\tau$, $l^+ = lu_\tau/\nu$ and $t^+ = tu_\tau^2/\nu$. However, the wall-normal distance for the lubricated channel is normalised somewhat different. Inside the film: $y^+ = yu_\tau/\nu_{\text{film}}$ where y is the distance from the nearest wall. The interface between the film and the bulk-fluid is then situated at $y^+_{\text{interface}} = 5$. In the bulk-fluid: $y^+ = y^+_{\text{interface}} + (y-h)u_\tau/\nu$. The results in the present study are extracted from a database consisting of 25 different instantaneous flow fields that were equally separated by $\Delta t^+ = 43.2$ in time.

3. Results and discussion

First, a conventional channel flow simulation is performed at a Reynolds number $Re_\tau = 180$, i.e. the pressure gradient is kept constant, which corresponds to a Reynolds number based on the mean velocity of $Re_m \approx 2800$. So far this simulation corresponds to the case considered by Kim et al. (1987). At $t^+ = 0$, however, the volumetric flow rate is frozen and the driving pressure gradient in the now lubricated channel is allowed to change. The sudden rise in pressure loss or drag at $t^+ = 0$ in Fig. 2 is because of the introduction of the lubricating film with viscosity twice that of the bulk-fluid at $t^+ = 0$. When the flow in the lubricated channel simulation has settled to a statistically steady state, a drag reduction of about 22% can be observed.

The mean velocity profiles in the conventional and the lubricated channel are shown (in wall units) in Fig. 3. Here, and throughout the rest of this paper, the lubricated and conventional channel flows are driven by exactly the same pressure gradients. The slope in the log-region of the lubricated channel is about the same as in the conventional channel. However, the log-region shows a substantial upward shift in the lubricated channel. This upward shift is commonly observed in turbulent flows with drag reduction (e.g. Choi et al., 1993, 1994). If we define the viscous sublayer as the region where $U^+/Y^+ > 0.95$ (i.e. almost linear), the sublayer thickness is increased from 5 in the conventional channel to about 9 wall units in the lubricated channel. When the displacement effect of the lubricating film is accounted for, the increase in flow rate (of the bulk-fluid) from the conventional to the lubricated channel is about 13.5%.

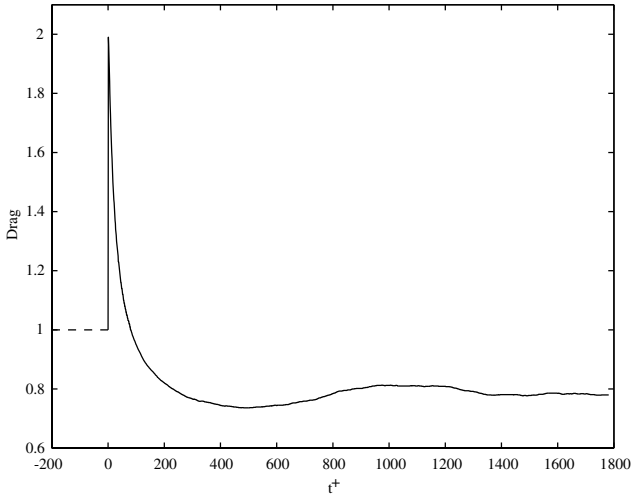

Fig. 2. Drag evolution ($\frac{dP}{dx_{\text{lub.}}} / \frac{dP}{dx_{\text{conv.}}}$) when the volumetric flow rate is kept constant. The lubricating film is inserted into the channel at $t^+ = 0$. —, Lubricated channel; – – –, conventional channel.

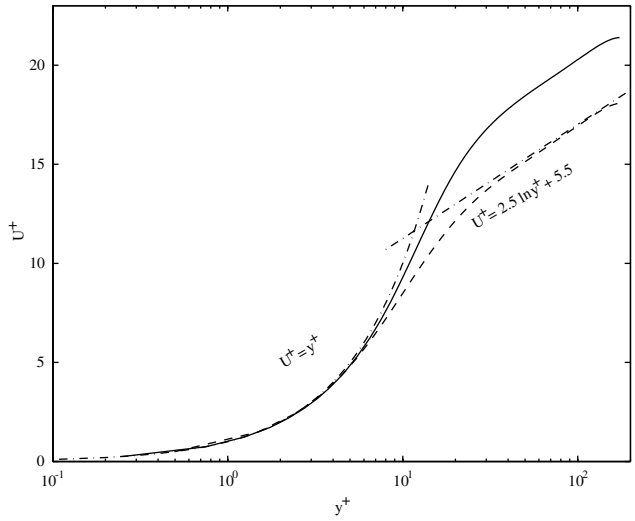

Fig. 3. Mean velocity profiles normalised in wall units. —, Lubricated channel; – – –, conventional channel.

Turbulence intensities (rms-values) are shown in Fig. 4(a). The major difference between the two data sets is the outward shift of the profiles in the lubricated channel. The outward shift is approximately equal to the film thickness h, which coincides with the increase of the viscous sublayer thickness. The wall-normal velocity fluctuations (v) are identically zero at the interface ($y = h$), i.e. vertical transport of momentum through the interface is prohibited. Thus the interface effectively reduces the interaction between the bulk-fluid and the solid wall by preventing inrush of high momentum fluid towards the wall (sweeps) and the transport of low

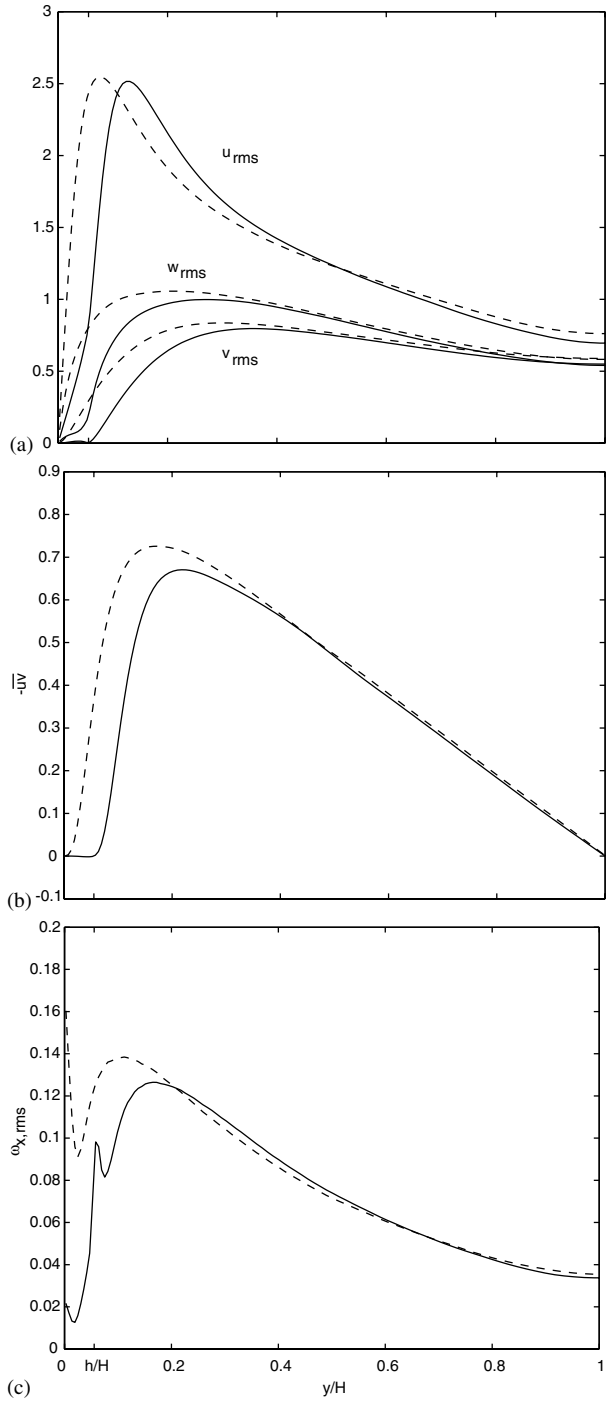

Fig. 4. (a) Root-mean-square velocity fluctuations. (b) Reynolds shear-stress. (c) Root-mean-square of streamwise vorticity. —, Lubricated channel; – – –, conventional channel. The innermost tick mark on the abscissa identifies the position of the interface.

momentum fluid away from the wall (ejections). This will ultimately lead to a reduction in Reynolds shear-stress in this region and $-\overline{uv}$ in Fig. 4(b) is in fact vanishing inside the lubricating film. The observed drag reduction can thus be explained by the reduction of $-\overline{uv}$ which is due to the reduced wall-normal transport of streamwise momentum, i.e. similar to the conclusions of Hammond et al. (1998) and Choi et al. (1994). It is noteworthy, however, that substantial fluid motions prevail parallel to the solid surface, in spite of the suppression of the wall-normal velocity inside the lubricating film.

To further explore the mechanisms responsible for the observed drag reduction in a lubricated channel, the focus of attention is now on the near-wall streamwise vortices. These vortices are, as noted in Section 1, responsible for a major part of the production of Reynolds stresses and, ultimately, for the excess skin-friction in turbulent wall flows. Furthermore, they are known to be situated in the buffer-region and are aligned predominantly in the streamwise direction (Jeong et al., 1997). Fig. 4(c) shows the root-mean-square streamwise vorticity fluctuations normalised by u_τ^2/ν. The local peak of ω_x in the interior of the channel is known to be associated with near-wall streamwise vortices (Kim et al., 1987). The peak in the lubricated channel shows an outward shift $\Delta y \approx h$. This strongly suggests that the lubricating film is displacing the near-wall vortical structures a distance comparable to the film thickness away from the wall. The peak value is about the same in the conventional and the lubricated channel, indicating that the strength of the vortices is about the same.

In order to capture these instantaneous flow structures we adopt the λ_2-vortex definition of Jeong and Hussain (1995). A vortex core is thus defined as a connected region of negative λ_2, which is the second largest eigenvalue of the tensor $s_{ik}s_{kj} + r_{ik}r_{kj}$ where $s_{ij} = (u_{i,j} + u_{j,i})/2$ is the strain-rate tensor and $r_{ij} = (u_{i,j} - u_{j,i})/2$ is the rotation tensor. Jeong et al. (1997) showed that this vortex definition is fully able to identify vortices in a turbulent channel flow. Vortices with different sign of streamwise vorticity are known to be equally probable and are also symmetric counterparts (Jeong et al., 1997). This investigation is accordingly limited to only those vortices with positive streamwise vorticity. In order to study the location and orientation of the vortices and the detailed topology of the skin-friction underneath them in the lubricated channel, an ensemble-averaging of the flow field around the streamwise vortices present in the instantaneous flow fields has been performed. The detection and averaging are based on the scheme devised by Jeong et al. (1997) to identify coherent vortices in the near-wall region of turbulent channel flow. The procedure consists of three steps: (i) Detection of vortical structures by the λ_2-definition conditioned on positive streamwise vorticity ω_x. (ii) Ensemble-averaging of the structures by aligning the midpoint of their streamwise length. In order to capture only fully grown structures the structures are required to have a streamwise length of at least $x^+ = 150$ in the region $15 < y^+ < 45$ ($10 < y^+ < 40$ for the conventional channel). (iii) Shifting of the alignment point to maxi-

mise the cross-correlation between the ensemble-averaged and the individual structures. Structures having a cross-correlation below 0.5 were discarded in order to reduce the smearing of the resulting coherent structure. The ensemble eventually consists of 279 instantaneous structures (273 for the conventional channel). The resulting structure can be considered a generic model of the instantaneous streamwise vortices and can accordingly be used to elucidate the dynamics of the turbulent wall flow (Jeong et al., 1997).

Figs. 5 and 6 show both a top view and a side view of the resulting ensemble-averaged coherent structure for the conventional and the lubricated channel, respectively. The contours in the background represent the associated ensemble-averaged wall-friction pattern normalised with the global mean skin-friction τ_{wall}. Fig. 6(a) clearly shows that the coherent structure in the lubricated channel is in fact lifted away from the wall, as was suggested by the rms-profile of the streamwise vorticity in Fig. 4(c). The actual distance that the structure is lifted closely corresponds to the film thickness (and the increase in viscous sublayer thickness). Even though the streamwise vorticity inside the film does not vanish, there is no sign of any vortical structures in this region. This is the main reason for the vanishing Reynolds shear-stress inside the film. The skin-friction pattern associated with the coherent structure in the conventional channel in Fig. 5(b) clearly shows a local region of exceptionally high skin-friction close to its tail. This is caused by the downwash of high-speed fluid by the structure itself (Choi et al., 1993; Kravchenko et al., 1993; Solbakken and Andersson, 2004). However, the structure in the lubricated channel in Fig. 6(b) is apparently not correlated with any such high skin-friction region. Modest variations in the skin-friction level do exist, but the deviation from the mean is less than 10%, while the maximum skin-friction in the conventional channel exceeds τ_{wall} by more than 50%.

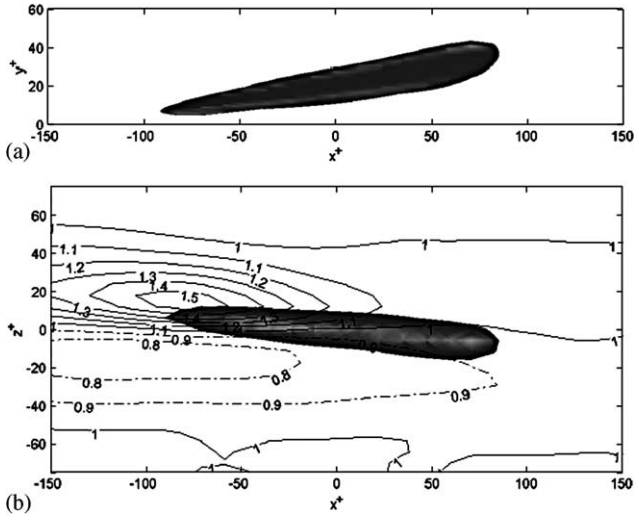

Fig. 5. Ensemble-averaged coherent vortex for the conventional channel. The shaded region shows an isosurface plot of $\lambda_2 = -0.01$. (a) Side view and (b) top view. The contour lines represent the associated coherent skin-friction normalised with the global mean skin-friction τ_{wall}.

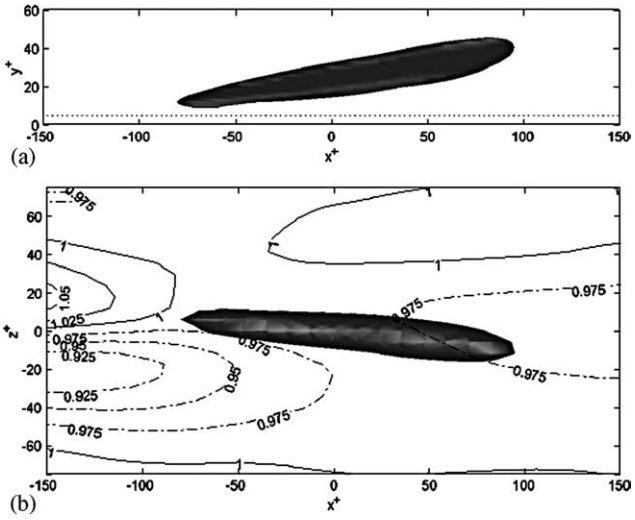

Fig. 6. Ensemble-averaged coherent vortex for the lubricated channel. The shaded region shows an isosurface plot of $\lambda_2 = -0.01$. (a) Side view and (b) top view. The contour lines represent the associated coherent skin-friction normalised with the global mean skin-friction τ_{wall}. The dotted line in (a) is the interface.

4. Feasibility

The purpose of the investigation presented herein is to examine how a turbulent bulk flow is affected by the presence of a thin lubricating liquid film. To enable accurate computer experiments based on first principles, i.e. direct numerical simulations of the Navier–Stokes equations, only low Reynolds number flows can be studied. Since the presence of waves on the interface between the bulk-fluid and the lubricant inevitably enhances the overall flow resistance, it is of the utmost importance to maintain a smooth interface. After having found that significant drag reduction does indeed occur in the low-Re computer experiments presented in the previous section, the crucial question arises whether or not the idealised situation with a wave-free interface can be realised in practise.

Let us for this purpose consider the transport of natural gas in long pipelines under high pressure. In a 1 m diameter pipeline operated at ~100 bar, the bulk velocity U_b is typically about 5 m/s, whereas the properties of the pressurised gas (mostly methane) are $\rho \approx 78$ kg/m^3 and $\mu \approx 1.4 \times 10^{-5}$ Ns/m^2. This gives a Reynolds number of about 2.8×10^7 based on U_b and the diameter D of the pipe, i.e. four orders of magnitude higher than the Reynolds number in the DNS. Coated pipelines for

transportation of natural gas over long distances have an equivalent sand–grain roughness of about 1 μm, i.e. close to being hydrodynamically smooth, and the Darcy friction factor f is approximately 7.2×10^{-3} according to the Moody chart. In the absence of a lubricating film, the associated pressure drop ΔP over a certain length L becomes:

$$\frac{\Delta P}{L}=\frac{f}{D}\frac{1}{2}\rho U_{\mathrm{b}}^2\approx 7.0\ \mathrm{Pa/m} \tag{2}$$

In pipe flow the total shear stress, i.e. viscous plus Reynolds stresses, varies linearly over the entire cross-section even in the presence of a lubricating film. The interfacial shear stress τ_i is thus directly related to the wall shear stress:

$$\tau_i=\tau_{\mathrm{wall}}\left(1-\frac{2h}{D}\right)\quad\text{where}\quad\tau_{\mathrm{wall}}=\frac{\Delta P}{L}\frac{D}{4} \tag{3}$$

Since the lubricating film is assumed to be thin compared to the diameter of the pipe, i.e. $h/D\ll 1$, the velocity inside the film varies nearly linearly with the distance from the wall as long as the Reynolds shear stress $-\overline{uv}$ is vanishingly small (as seen in Fig. 4(b)). The interfacial velocity u_i can therefore be approximated as:

$$u_i=\frac{\tau_i h}{\mu_{\mathrm{film}}}=\frac{\Delta P}{L}\frac{D}{4\mu_{\mathrm{film}}}\left(1-\frac{2h}{D}\right)h \tag{4}$$

Let us furthermore assume that the lubricating liquid is water at ~20 °C and ~100 bar and with density $\rho_{\mathrm{film}}\approx 1000\ \mathrm{kg/m^3}$ and $\mu_{\mathrm{film}}\approx 1.0\times10^{-3}\ \mathrm{Ns/m^2}$. The interfacial tension between the dense gas phase and water is $\sigma\approx 4.4\times10^{-2}$ N/m. In this particular example the kinematic viscosity of the liquid film is about 5.6 times larger than that of the pressurised gas. With these parameter values, and with the interfacial velocity obtained from Eq. 4, the criterion for interfacial stability (that the Weber number defined in Eq. 1 should not exceed 3) suggests that the interface between the thin water film and the pressurised natural gas remains smooth as long as the film thickness $h\lesssim 0.35$ mm.

5. Concluding remarks

The present exposition has demonstrated that a significant drag reduction is possible to achieve in a lubricated turbulent channel flow. The fluid–fluid interface prevents wall-normal transport of momentum, and the near-wall streamwise vortices are thereby pushed further into the flow. As a result the thin lubricating film is essentially free of turbulent shear-stresses and the viscous sublayer thickness is increased. The lubricating film furthermore prevents local regions of high skin-friction from developing. This is mainly due to the reduced interaction between the wall and the bulk-fluid in which the streamwise vortices are present. These observations explain the achieved drag reduction.

The substantial drag reduction observed is inherently associated with the assumption of a wave-free interface between the lubricant and the core flow. It is intuitively clear that the thickness h of the lubricating film should be substantially smaller than the hydraulic radius H of the channel or pipe considered in order to prevent the formation of interfacial waves. To facilitate the maintenance of a smooth interface, stability-promoting agents may furthermore be added to the lubricant (Rojey et al., 1999).

Acknowledgements

This work has received support from The Research Council of Norway (Programme for Supercomputing) through a grant of computing time. The MGLET code was generously made available by Prof. H. Wengle (Universität der Bundeswehr München) and Prof. R. Friedrich (Technische Universität München). The constructive comments of the reviewers helped to improve the final version of this paper and encouraged us to include the section on feasibility.

References

Choi, H., Moin, P., Kim, J., 1993. Direct numerical simulation of turbulent flow over riblets. J. Fluid Mech. 255, 503–539.

Choi, H., Moin, P., Kim, J., 1994. Active turbulence control for drag reduction in wall-bounded flows. J. Fluid Mech. 262, 75–110.

den Toonder, J.M.J., Hulsen, M.A., Kuiken, G.D.C., Nieuwstadt, F.T.M., 1997. Drag reduction by polymer additives in a turbulent pipe flow: numerical and laboratory experiments. J. Fluid Mech. 337, 193–231.

Endo, T., Himeno, R., 2002. Direct numerical simulation of turbulent flow over a compliant surface. J. Turbulence 3, 007.

Hammond, E.P., Bewley, T.R., Moin, P., 1998. Observed mechanisms for turbulence attenuation and enhancement in opposition-controlled wall-bounded flows. Phys. Fluids 10, 2421–2423.

Jeong, J., Hussain, F., 1995. On the identification of a vortex. J. Fluid Mech. 285, 69–94.

Jeong, J., Hussain, F., Schoppa, W., Kim, J., 1997. Coherent structures near the wall in a turbulent channel flow. J. Fluid Mech. 332, 185–214.

Joseph, D.D., Bai, R., Chen, K.P., Renardy, Y.Y., 1997. Core-annular flows. Annu. Rev. Fluid Mech. 29, 65–90.

Kang, S., Choi, H., 2000. Active wall motions for skin-friction drag reduction. Phys. Fluids 12, 3301–3304.

Kim, J., 1992. Study of turbulence structure through numerical simulations: the perspective of drag reduction. AGARD report (R-786), AGARD FDP/VKI Special Course on Skin Friction Drag Reduction, Chapter 7, 2–6 March 1992,VKI, Belgium, pp. 1–14.

Kim, J., Moin, P., Moser, R., 1987. Turbulence statistics in fully developed channel flow at low Reynolds number. J. Fluid Mech. 177, 133–166.

Kravchenko, A.G., Choi, H., Moin, P., 1993. On the relation of near-wall streamwise vortices to wall skin friction in turbulent boundary layers. Phys. Fluids A 5, 3307–3309.

Lee, C., Kim, J., 2002. Control of the viscous sublayer for drag reduction. Phys. Fluids 14, 2523–2529.

Lee, C., Kim, J., Babcock, D., Goodman, R., 1997. Application of neural networks to turbulence control for drag reduction. Phys. Fluids 9, 1740–1747.

Manhart, M., Tremblay, F., Friedrich, R., 2001. MGLET: a parallel code for efficient DNS and LES of complex geometries. In: Parallel Computational Fluid Dynamics—Trends and Applications. Elsevier, pp. 449–456.

Miesen, R., Boersma, B.J., 1995. Hydrodynamical stability of a sheared liquid film. J. Fluid Mech. 301, 175–202.

Miles, J.W., 1960. The hydrodynamical stability of a thin film of liquid in uniform shearing motion. J. Fluid Mech. 8, 593–610.

Orellano, A., Wengle, H., 2000. Numerical simulation (DNS and LES) of manipulated turbulent boundary layer flow over a surface-mounted fence. Eur. J. Mech. B—Fluids 19, 765–788.

Orlandi, P., 1995. A tentative approach to the direct simulation of drag reduction by polymers. J. Non-Newtonian Fluid Mech. 60, 277–301.

Orlandi, P., Fatica, M., 1997. Direct simulations of turbulent flow in a pipe rotating about its axis. J. Fluid Mech. 343, 43–72.

Robinson, S.K., 1991. Coherent motions in the turbulent boundary layer. Annu. Rev. Fluid Mech. 23, 601–639.

Rojey, A., Palermo, T., Falcimaigne, J., 1999. Method of transporting gas under pressure in the presence of a liquid film. US Patent 5 983 915.

Satatke, S., Kasagi, N., 1996. Turbulence control with wall-adjacent thin layer damping spanwise velocity fluctuations. Int. J. Heat Fluid Flow 17, 343–352.

Schoppa, W., Hussain, F., 1998. A large-scale control strategy for drag reduction in turbulent boundary layers. Phys. Fluids 10, 1049–1051.

Smith, M.K., Davis, S.H., 1982. The instability of sheared liquid layers. J. Fluid Mech. 121, 187–206.

Solbakken, S., Andersson, H.I., 2004. The generic skin-friction pattern underneath coherent near-wall structures. Fluid Dyn. Res. 34, 167–174.

Sumitani, Y., Kasagi, N., 1995. Direct numerical simulation of turbulent transport with uniform wall injection and suction. AIAA J. 33, 1220–1228.